Nanostructured zinc doped tungsten oxide films for antibacterial applications

R. Ravi Kumar [a], P. J. Khan [a], D. S. Rao [a], G. Kalpana [a], A. Sivasankar Reddy [a,*], P. Gopikrishna [b], A. M. Krishna [c], P. S. Reddy [d]
[a] *Department of Physics, Vikrama Simhapuri University College, Nellore-524320, Andhra Pradesh, India*
[b] *Department of Zoology, Vikrama Simhapuri University College, Kavali-524201, Andhra Pradesh, India*
[c] *Central Instrumentation Centre, Vikrama Simhapuri University College, Nellore-524320, Andhra Pradesh, India*
[d] *Department of Physics, Sri Venkateswara University, Tirupati-517502, Andhra Pradesh, India*

Pure and zinc doped tungsten oxide films were deposited on glass substrates at various wt% of zinc by using the electron beam evaporation method. The scanning electron microscope (SEM), X-ray photoelectron spectroscopy (XPS), and UV-Vis-NIR double beam spectrometry techniques were used to assess the properties of pure and zinc doped tungsten oxide films. From the SEM results, undoped tungsten oxide films exhibited a rice hull type nanostructure. The zinc doped tungsten oxide films exhibited a spider net structure. The antibacterial activity of Zn-WO_3 films was studied with Pseudomonas aeruginosa. The zinc doped WO_3 films are effectively inhibiting the bacteria's growth.

(Received October 28, 2024; Accepted January 14, 2025)

Keywords: Tungsten oxide, Thin films, Nanocrystalline, Antibacterial

1. Introduction

In the interdisciplinary research area, nanostructured materials play a key role due to its physical, chemical, electrical and optical properties, and the nanostructure may increase the performance of any material in technological aspects [1]. Researchers are working for the preparation of different types of nanostructures to make them more efficient gas sensors and antibacterial activities. Antibacterial coatings play a key role in biomedical purposes such as medical devices, surgery tools, human implants, etc. Metal nanoparticles exhibited excellent antibacterial activities, but to avoid the associated problems with metals as antibacterial material, researchers focused on metal oxides as antibacterial materials due to its unique properties [2]. The antibacterial activity of metal oxide has been investigated by various research groups using different materials such as Cu_2O, TiO_2, ZnO, SnO_2, and WO_3 by various synthesis approaches [3]. Among these metal oxides, tungsten oxide (WO_3) has attracted great interest due to its unique properties such as wide band gap, photocatalytic activity, good stability against acidic media, and excellent electron conductivity [4-6]. Pure and doped WO_3 thin films are prepared using several methods, such as electron beam evaporation [7], sputtering [8], resistivity heating [9], spray pyrolysis deposition [10], and spin-coating [11]. In this work, WO_3 and Zn-WO_3 films were prepared by using electron beam evaporation, and the antibacterial activity of the films was tested against *Pseudomonas aeruginosa* by using the pour plate method. To the best of our knowledge, up to now, there is no report on the electron beam evaporated Zn doped WO_3 thin films for antibacterial (*Pseudomonas aeruginosa*) applications.

* Corresponding author: akepati77@gmail.com
https://doi.org/10.15251/JOBM.2025.171.9

2. Experimental

Pure tungsten oxide (WO_3) and Zinc-doped tungsten oxide (Zn-WO_3) pellets were used to prepare nanostructured thin films on glass substrates by electron beam evaporation technique. WO_3 and Zn-WO_3 pellets were prepared using high purity (99.99%) of WO_3 and Zn powders. The films were deposited at room temperature and the thicknesses of the films were approximately 260 nm.

2.1. Characterization of WO_3 and Zn-WO_3 nanostructured films

The microstructure was analyzed by scanning electron microscopy (SEM). The chemical composition was studied using X-ray photoelectron spectroscopy (XPS). The optical properties of the films were recorded by UV-Vis-NIR double beam spectrometry.

3. Results and discussions

3.1. Microstructure

The SEM images of WO_3 and Zn-WO_3 nanostructured films are shown in Fig.1. The WO_3 films show the nanoflakes that were uniformly distributed on the surface of the substrate (Fig. 1(a)), and the continuity of these nanoflakes is increased after doping with 5 wt% of Zn (Fig. 1(b)). This structure is gradually changed into a spider nest like structure at the films doped with 10 wt% of Zn (Fig. 1(c)). Beyond this doping concentration, the films exhibited a dense structure (Fig. 1(d)). The doping of Zn to WO_3 accelerated the surface and interlaminar diffusions of deposited atoms. Hence, it allows to create a compact structure at higher doping concentration WO_3 films. From the SEM results, the microstructure of the WO_3 films is highly influenced by the doping concentration of Zn.

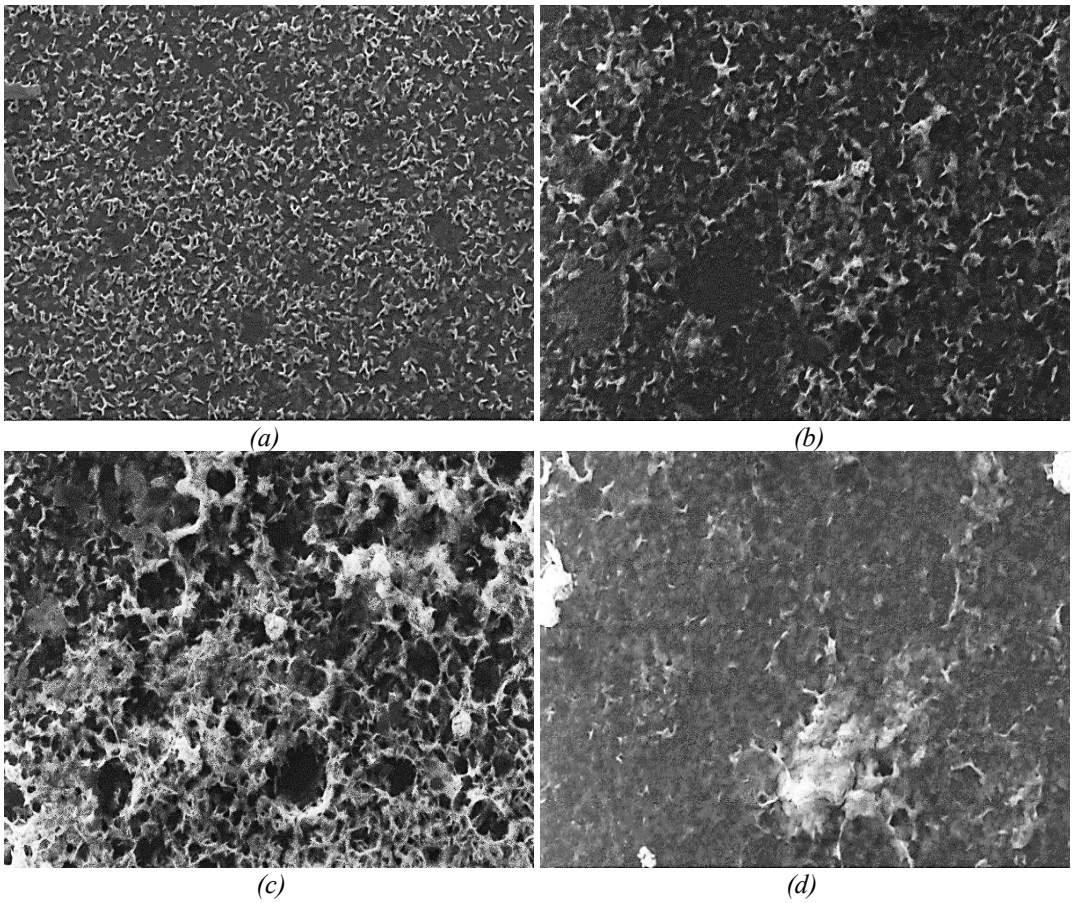

Fig. 1. SEM images: (a) WO_3 (b) 5wt% Zn doped (c) 10wt% Zn doped (d) 15wt% Zn doped WO_3 films.

3.2. XPS analysis

The chemical states and composition of Zn-WO_3 nanostructure films were studied using XPS. Fig.2. shows the chemical states of the Zn doped WO_3 nanostructured films. The 4f spectrum of W is shown in Fig. 2 (a) and is presented as a spin-orbit doublet of W4f7/2 and W4f5/2 for the valance state of W. Two intense peaks are centered at 35.41 eV and 37.53 eV, which correspond to the W 4f7/2 and W 4f5/2 doublets, respectively. The obtained values are in good agreement with the literature of W^{6+} in stoichiometric WO_3 by Navio et al. [13]. Fig. 2(b) shows the O 1s spectrum, and a peak is located at 529.2 eV, which is related to the O^{2-} peak. Fig. 2(c) shows the Zn 2p spectrum, which consists of a peak at 1019.9 eV, which corresponds to the binding energies of Zn2p3/2, and can be attributed to zinc metal.

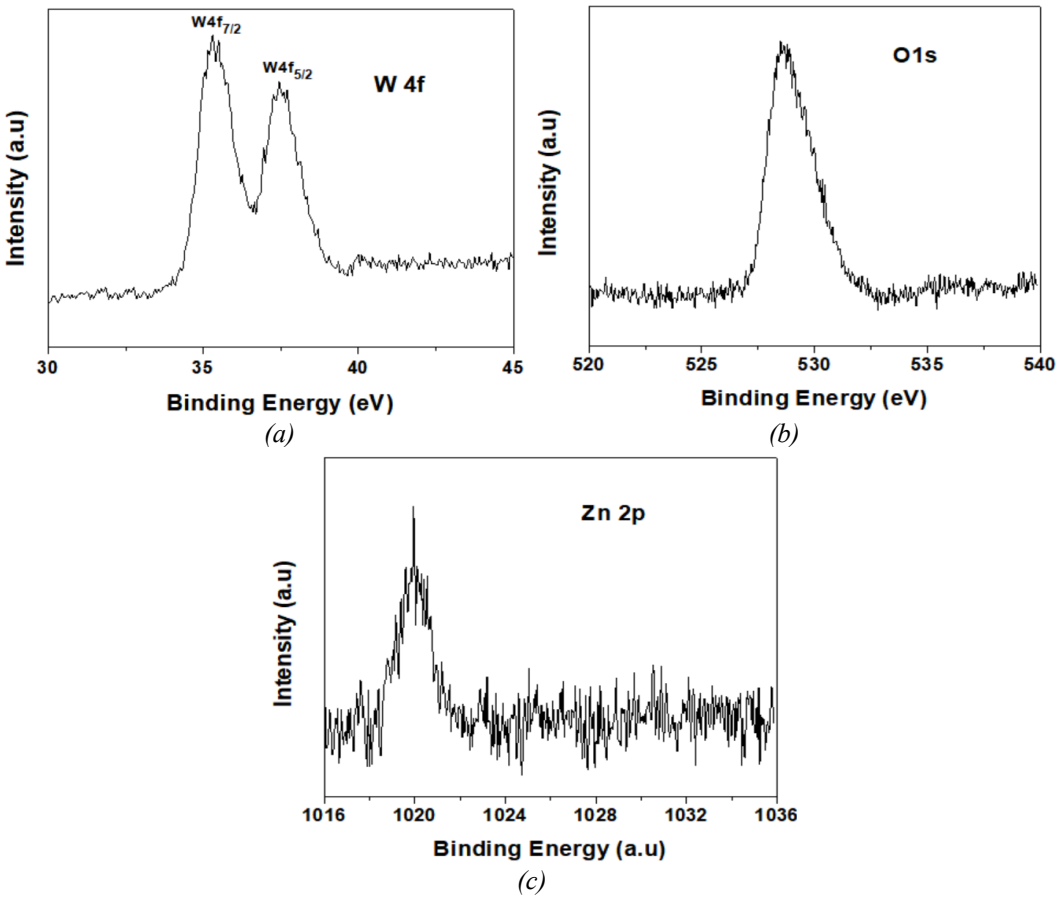

Fig. 2. XPS spectra of Zn-WO_3 nanostructure films with a 10wt% Zn doped: (a) W4f, (b) O1s, and (c) Zn 2p.

3.3. Optical properties

Figure 3 shows the optical transmittance spectrum of nanostructured WO_3 and Zn-WO_3 films. The average optical transmittance of the films was around 85% in the visible region. The optical transmittance decreased after adding zinc to tungsten oxide. However, 15wt%Zn doped WO_3 films exhibited higher transmittance than the WO_3 films, and this may be due to changes in the microstructural properties of the films.

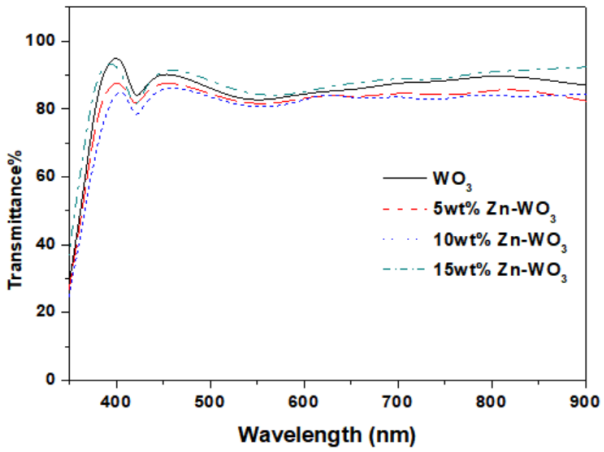

Fig. 3. Optical transmittance spectrum of WO_3 and Zn-WO_3 nanostructure films.

The estimated value of the bandgap from the intercept on the energy axis of the linear portion of Tauc plot for WO_3 thin films lies in the range of 3.19 to 3.32eV. The bandgap was found to decrease from 3.28 to 3.19eV from WO_3 to 10wt% of zinc doped WO_3 films. However, 15wt% zinc doped WO_3 films show the highest bandgap of 3.32eV. The present obtained bandgap values for WO_3, 5 wt% Zn-WO_3, 10 wt% Zn-WO_3 and 15 wt% Zn-WO_3 are 3.29 eV, 3.26 eV, 3.19 eV and 3.32eV, respectively. The larger band gap observed for the deposited thin films can be attributed to their amorphous nature [14]. Hendi et al. [15] recorded that the bandgap of WO_3 films decreased from 3.30 eV to 2.47eV with an increase in the CdTe doping concentration from 0 to 25%.

3.4. Antimicrobial activity

3.4.1. Test organism & growth conditions:

Pseudomonas aeruginosa (MTCC 424) a gram-negative bacterium was obtained from the Microbial Type Culture Collection, Chandigarh, India. *Pseudomonas aeruginosa* is cultured under standard laboratory conditions in LB media at 30^0C. The overnight culture was used in this experiment.

The antimicrobial activity of the nanostructured WO_3 and Zn-WO_3 was evaluated by the pour plate method [16] with slight modification by using LB agar media (Hi-media, India), the microorganisms being tested were grown on LB broth media. Briefly, *Pseudomonas aeruginosa* (*P. aeruginosa)* was grown on LB broth at 30°C overnight, a loop full of the growth was then inoculated into Mueller Hinton broth (Thermo Scientific) and incubated at 30°C on a rotary shaker until the turbidity of the growth was equivalent to the density of 0.5 McFarland standard. The microorganism was then either inoculated (0.25 mL) into molten MHA and poured into petri dishes (pour plate technique).

The antibacterial properties of the nanostructured WO_3 and Zn-WO_3 films are shown in Fig.4. The antibacterial activity of the WO_3 and Zn-WO_3 films was evaluated against P. *aeruginosa. P. aeruginosa* is an opportunistic pathogen belongs to gram-negative bacteria which, causes concern for humanity. The pour plate technique was used to test the antibacterial activity of the WO_3 based films. WO_3 and 10wt% Zn-WO_3 films were used to determine the antibacterial activity. The results demonstrate that pure WO_3 films fail to inhibit the growth of bacteria (Fig.4(a)), whereas, 10wt% Zn-WO_3 films inhibit the growth of *P. aeruginosa* (Fig.4(b)). After culture, the bacteria spread around the plate, except the area of Zn-WO_3 coating. The antibacterial activity of WO_3 films increases after adding the 10wt% zinc doping to WO_3. From this result, we found that Zn-WO_3 has the potential to be used as an antibacterial coating against *P. aeruginosa*.

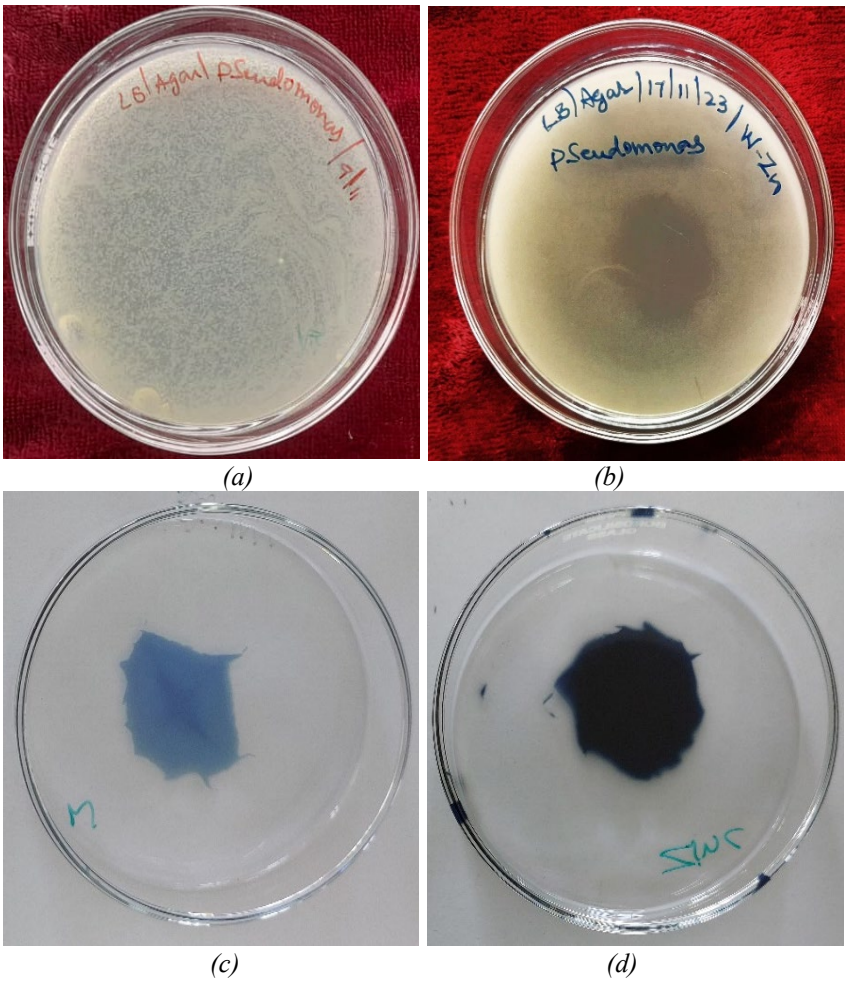

Fig. 4. Antibacterial properties: (a) WO_3 films, (b) 10wt% Zn- WO_3 films, (c) uncultured WO_3 films and (d) uncultured 10wt% Zn- WO_3 films.

4. Conclusions

The spider nest like nanostructured WO_3 based films were prepared by the electron beam evaporation method on glass substrates. From the SEM results, the microstructure of the WO_3 films was highly influenced by the doping concentration of Zn. The films nanostructure changed from nanoflakes to the spider nest like structure after adding the 10wt%Zn to WO_3. The addition of Zn accelerated the diffusion of deposited atoms, consequently, the surface morphology changed. Zn-doped WO_3 films were found to inhibit the growth of tested bacteria. It is observed that the Zn dopant brings the best result in the antibacterial activity of WO_3 films. The combined use of WO_3 based nanostructure films with biology is expected to fabricate significant advances in the field of antibacterial coatings.

References

[1] A. Mubayi, S. Chatterji, P. Rai, G. Watal, Adv. Mater. Lett. 3 (6), 519 (2012); https://doi.org/10.5185/amlett.2012.icnano.353

[2] Abbad Al Baroot, Q.A. Drmosh, Ibrahim Olanrewaju Alade, Khaled A. Elsayed, Muidh Alheshibri, Essam Kotb, H.R. AlQahtani, Hassan S. Al Qahtani, Optical Materials 133, 112886 (2022); https://doi.org/10.1016/j.optmat.2022.112886

[3] Guang-Lei Tan, Dan Tang, Davoud Dastan, Azadeh Jafari, Zhicheng Shi, Qian-Qian Chu, Jos'e P.B. Silva, Xi-Tao Yin Ceramics International 47 (12), 17153 (2021); https://doi.org/10.1016/j.ceramint.2021.03.025

[4] C.M. Ling, L. Yuliati, H.O. Lintang, S.L. Lee, Malaysian J. Chem. 22 (2), 29 (2020).

[5] Y. Yun, J.R. Araujo, G. Melaet, J. Baek, B.S. Archanjo, M. Oh, A.P. Alivisatos, G. A. Somorjai,Catal. Lett. 147 (3), 622 (2017); https://doi.org/10.1007/s10562-016-1915-2

[6] T. Zheng, W. Sang, Z. He, Q. Wei, B. Chen, H. Li, C. Cao, R. Huang, X. Yan, B. Pan, S. Zhou,Nano Lett. 17 (12), 7968 (2017); https://doi.org/10.1021/acs.nanolett.7b04430

[7] Adilakshmi Griddaluru, Sivasankar Reddy Akepati, ChemPhysMater 2 (2), 172 (2023); https://doi.org/10.1016/j.chphma.2022.09.003

[8] G V .A. Reddy, K.N. Kumar, S.A. Sattar, H.D. Shetty, N.G. Prakash, R.I. Jafri, C. Devaraja, B C. Manjunatha, C S Kaliprasad , R. Premkumar, S. Ansa, Physica B: Condensed Matter 664, 414996 (2023); https://doi.org/10.1016/j.physb.2023.414996

[9] Fabien Sanchez, L. Marot, A. Dmitriev, R. Antunes, R. Steiner, E. MeyerJournal of Alloys and Compounds 968, 171888 (2023); https://doi.org/10.1016/j.jallcom.2023.171888

[10] V. Ganbavle, S. Shaikh, S. Mohite, S. Inamdar, A Bagade, A. Patil, K. Rajpure, Chemical Physics Letters 814, 140327 (2023); https://doi.org/10.1016/j.cplett.2023.140327

[11] Ümit Özlem Akkaya Arıer, Optik 262, 169195 (2022); https://doi.org/10.1016/j.ijleo.2022.169195

[12] Chen ZW, Lai JKL, Shek CH. J Non-Cryst Solids 355(52-54), 2647 (2009); https://doi.org/10.1016/j.jnoncrysol.2009.09.001

[13] C Navío, S Vallejos, T Stoycheva, E Llobet, X Correig, R Snyders, C Blackman, P Umek,X Ke, G Van Tendeloo, C Bittencourt, Mater. Chem. Physics 134(2-3), 809 (2012); https://doi.org/10.1016/j.matchemphys.2012.03.073

[14] M Mazur, D Wojcieszak, A Wiatrowski, D Kaczmarek, A Lubanska, J Domaradzki, Appl. Surf. Sci. 570, 151151 (2021); https://doi.org/10.1016/j.apsusc.2021.151151

[15] A.H.Y. Hendi, M.F. Al-Kuhaili, S.M.A. Durrani, M.M. Faiz, A. Ul- Hamid, A. Qurashi, I. Khan, Material Research Bulletin 87, 148 (2017); https://doi.org/10.1016/j.materresbull.2016.11.032

[16] International Organization for Standardization. 2014. ISO 4833-1:2014.